Case Report

# *In situ* right posterior sectionectomy during liver procurement based on preoperative 3D planning to prevent extreme large-for-size syndrome in adult-to-adult liver transplantation: a case report

**Shiran Zhang, Bo Zhou, Ping Chen, Geng Chen^**

Department of Hepatobiliary Surgery, Daping Hospital, Army Medical University, Chongqing, China

*Contributions:* (I) Conception and design: G Chen, P Chen; (II) Administrative support: G Chen; (III) Provision of study materials or patients: S Zhang, G Chen; (IV) Collection and assembly of data: B Zhou; (V) Data analysis and interpretation: S Zhang, B Zhou; (VI) Manuscript writing: All authors; (VII) Final approval of manuscript: All authors.

*Correspondence to:* Geng Chen, MD, PhD, Department of Hepatobiliary Surgery, Daping Hospital, Army Medical University. No. 10, Changjiang Branch Road, Daping, Yuzhong District, Chongqing 400042, China. Email: chengeng@tmmu.edu.cn.

**Background:** Large-for-size syndrome (LFSS) is an uncommon but potentially lethal complication following adult liver transplantation (LT). Reduced-size liver transplantation (RSLT) is considered a valuable alternative to delayed fascial closure or mesh closure for preventing LFSS. In this article, we report a successful adult-to-adult RSLT case with *in situ* right posterior graft sectionectomy using three-dimensional (3D) computer-assisted planning. This case is unique, as it employed preoperative planned *in situ* right posterior segmental resection (iRPS).

**Case Description:** A short and slim, 69-year-old woman was admitted to Daping Hospital in January, 2023. The patient had previously been diagnosed with hepatitis B virus (HBV)-related hepatocellular carcinoma and acute-on-chronic liver failure. She had received 1 month of hepatoprotective and anti-HBV treatment before being admitted to Daping Hospital, and she had not suffered from any episodes of encephalopathy or upper gastrointestinal bleeding. The physical examination revealed moderate yellow staining of the skin and sclera, abdominal distension, shifting dullness, and pitting edema of the lower limbs. The laboratory test results revealed high serum total bilirubin (TBil) (121.2 μmol/L) and a long prothrombin time (PT) (23.4 s). Computed tomography (CT) showed a 3.4 cm × 2.9 cm nodule in segment V of the liver without macrovascular invasion. Due to the patient's poor liver function, conventional anti-tumor therapies (e.g., surgical resection, transcatheter arterial chemoembolization, and radiofrequency ablation) could not be used, and LT was the only feasible treatment for the patient. The graft volume (GV) of the allocated liver was measured by computed tomography volumetry (CTV). The estimated graft-recipient weight ratio (GRWR) was 3.8%, and the estimated graft weight/right anteroposterior ratio (GW/RAP) was 120.2, which indicated that the donor liver size was severely mismatched with the recipient's abdominal cavity. After meticulous surgical planning using a 3D simulation implanting model, an *in situ* right posterior graft sectionectomy was performed, and the reduced-size graft was successfully implanted in the recipient. The post-transplant course was uneventful. At the 12-month follow-up, the patient had an excellent quality of life, and no signs of tumor recurrence.

**Conclusions:** In situ right posterior graft sectionectomy is a feasible and effective strategy for preventing LFSS, especially if there is a size discrepancy between the donor liver anteroposterior dimensions and the recipient's lower right hemithorax. Accurate preoperative surgical planning is the key element in the success of the proposed size-reduction strategies.

^ ORCID: 0000-0002-1642-7098.

**Keywords:** Posterior sectionectomy; three-dimensional planning (3D planning); large-for-size syndrome (LFSS); liver transplantation (LT); case report

Submitted Mar 13, 2024. Accepted for publication Oct 21, 2024. Published online Nov 29, 2024.
doi: 10.21037/qims-24-507
**View this article at:** https://dx.doi.org/10.21037/qims-24-507

## Introduction

Large-for-size syndrome (LFSS) after liver transplantation (LT) can be lethal due to vascular complications and graft necrosis induced by rib compression. LFSS has been widely described in pediatric LT (1). However, given the increased prevalence of obesity among the donor population and the urgent need for liver grafts (i.e., urgent re-transplantation due to fulminant liver failure), the occurrence of LFSS is likely to increase among adult LT patients (2).

Currently, the system for allocating organs primarily focuses on the degree of liver disease severity rather than the physical characteristics of both the donor and the recipient. Therefore, transplant surgeons can face graft-recipient size mismatch (GRSM) in adult LT patients. Reduced-size liver transplantation (RSLT) has been considered an effective solution for LFSS. Under this procedure, the graft is trimmed to fit the abdominal cavity of the recipient, and meticulous surgical planning usually determines the success of the proposed strategy (3). In this article, we report a successful case of adult-to-adult RSLT with *in situ* right posterior graft sectionectomy that preserved the right hepatic vein (RHV), in which three-dimensional (3D) computer-assisted preoperative planning was used. We present this case in accordance with the CARE reporting checklist (available at https://qims.amegroups.com/article/view/10.21037/qims-24-507/rc).

## Case presentation

All procedures performed in this study were in accordance with the ethical standards of the institutional and/or national research committee(s) and with the Helsinki Declaration (as revised in 2013). Written informed consent was obtained from the patient for the publication of this case report and any accompanying images. A copy of the written consent is available for review by the editorial office of this journal.

The patient was a short and slim, 69-year-old woman (*Table 1*). She had previously been diagnosed with hepatitis B virus (HBV)-related hepatocellular carcinoma and acute-on-chronic liver failure. She had received 1 month of hepatoprotective and anti-HBV treatment before being admitted to Daping Hospital in January, 2023. She had not suffered from any episodes of encephalopathy or upper gastrointestinal bleeding.

The physical examination revealed moderate yellow staining of the skin and sclera, abdominal distension, shifting dullness, and pitting edema of the lower limbs. The laboratory test results were as follows: alanine aminotransferase (ALT), 43.3 IU/L (normal range, 0–40 IU/L); aspartate aminotransferase (AST), 88.6 IU/L (normal range, 0–40 IU/L); total bilirubin (TBil): 121.2 μmol/L (normal range, 3.4–17.1 μmol/L); alpha-fetoprotein (AFP), 2745 ng/mL (normal range, 0–25 ng/mL); international normalized ratio (INR), 2.04 (normal range, 0.8–1.5); prothrombin time (PT), 23.4 s (normal range, 11–13 s); and fibrinogen (Fib), 1.53 g/L (normal range, 2–4 g/L).

The computed tomography (CT) showed a 3.4 cm × 2.9 cm nodule in segment V of the liver without macrovascular invasion (*Figure 1A,1B*). Intra- and extra-hepatic metastasis was ruled out by positron emission tomography/CT. The patient had a Child-Pugh score of 9, and a Model for End-Stage Liver Disease score of 22. The preoperative assessment confirmed that the patient met the Milan or University of California San Francisco (UCSF) criteria (4). Due to the patient's poor liver function, conventional anti-tumor therapies (e.g., surgical resection, transcatheter arterial chemoembolization, and radiofrequency ablation) could not be used, and LT was the only feasible treatment for the patient.

The allocated liver graft was from a 65-year-old man in the intensive care unit of Daping Hospital who was brain dead with irreversible brain damage secondary to cerebral hemorrhage (*Table 1*). His liver function test and INR were normal. The whole graft volume (GV) measured by computed tomography volumetry (CTV) was 2,049.2 mL (*Figures 1C-1H*). According to the liver volume-to-weight conversion formulas [right lobe: estimated graft weight (eGW, g) =143.704 + 0.678 × CTV – measured GV (mL);

 

**Table 1** The demographic and morphometric data of the recipient and the allocated donor

| Variables | Recipient | Donor |
|---|---|---|
| Patient characteristics | | |
| Sex | Female | Male |
| Age (years) | 69 | 65 |
| Weight (kg) | 43.7 | 72 |
| Height (cm) | 153 | 170 |
| BMI (kg/m$^2$) | 18.7 | 24.6 |
| Morphometric data | | |
| Whole liver volume (mL) | 779.5 | 2,049.2 |
| Right lobe volume (mL) | NA | 1,691.0 |
| Left lobe volume (mL) | NA | 358.2 |
| Right posterior lobe volume (mL) | NA | 791.3 |
| Estimated whole liver weight (g) | 672.2 | 1,647.0 |
| Estimated right lobe weight (g) | NA | 1,290.2 |
| Estimated left lobe weight (g) | NA | 356.8 |
| Estimated right posterior lobe weight (g) | NA | 680.2 |
| Estimated remnant graft weight (g) | NA | 966.8 |
| Actual whole liver weight (g) | 685.7 | 1,602.8 |
| Actual right posterior lobe weight (g) | NA | 736.0 |
| Actual remnant graft weight (g) | NA | 866.8 |
| RAP distance (cm) | 13.7 | 18.5 |
| AP distance (cm) | 8.0 | 10.0 |
| SS distance (cm) | 22.8 | 28.8 |

BMI, body mass index; RAP, right anteroposterior; AP, anteroposterior; SS, side-to-side; NA, not available.

left lobe: eGW (g) = 41.63 + 0.88 × CTV – measured GV (mL)] (5,6), the eGW of the graft was 1,647.0 g, and the estimated graft-recipient weight ratio (GRWR) was 3.8%. The estimated graft weight/right anteroposterior ratio (GW/RAP) was 120.2. Previous studies have reported that a GRWR >2.5% and a GW/RAP >100 are associated with a size discrepancy between the donor liver and the recipient's abdominal cavity (3), which might lead to a higher risk of LFSS; thus, a graft split or reduction was needed in this case (*Table 2*).

Preoperative surgical planning was performed using a 3D simulation implanting model developed using commercial 3D reconstruction software (Smart Vision 3DVWorks, Smart Vision Ltd., Shenzhen, China). Preoperative CT images of the donor and recipient were used for the 3D reconstruction and calculation of the GV. The eGW of the left liver graft was 356.8 g, accounting for only 21.7% of the whole graft weight. The RAP of the donor (18.5 cm) was much longer than that of the recipient (13.7 cm). Limited resection, such as left lateral lobectomy or left hemihepatectomy, cannot relieve the compression of the right liver graft due to the ribs (*Figure 2A-2D*). Right hemihepatectomy may lead to small-for-size syndrome (SFSS) due to an insufficient future liver remnant. The eGW of the right posterior lobe of the liver graft was 680.2 g, accounting for 41.3% of the whole liver weight. After right posterior graft sectionectomy, it was estimated the GRWR would decrease to 2.2%, and the estimated GW/RAP would decrease to 70.6, which would meet the needs of the recipient and prevent LFSS.

Our 3D simulation implanting model revealed that after size reduction and slight posterior rotation around the inferior vena cava (IVC) of the remaining graft, the donor liver would fit the recipient's right upper abdominal cavity very well (*Figure 2E-2H*). The portal territory analysis revealed that segment 7 was supplied by branches from the right posterior portal vein, and segment 6 was supplied by branches from the right anterior portal vein. The same issue arose with the hepatic artery and the bile ducts. Therefore, the liver was not suitable for right posterior sector graft procurement (*Figure 3A*). However, given that it would be difficult for the recipient to continue waiting for a more suitable donor liver due to the rapid progression of her disease, we accepted the donor liver and prepared for the LT.

The *in situ* right posterior graft sectionectomy was then performed (*Figure 3B-3F*). After entering the abdomen, the right lobe of the graft was fully dissociated. Doppler ultrasound was used to determine the course of the RHV, which was marked on the liver surface using electrocoagulation. The liver parenchyma was transected along the right side of the RHV from the foot side of the donor liver with an ultrasonic scalpel (Harmonic Ace+7, 5 mm Diameter Shears with Advanced Hemostasis, Ethicon Endo-Surgery, Ciudad Juarez, Chihuahua, Mexico) without blocking the portal blood flow. Intrahepatic ducts with a diameter >3 mm were either tied off or secured with clips. The right posterior hepatic pedicle and RHV were transected using a line stapler (Ethicon Endo-Surgery, Cincinnati, Ohio, USA). Hemostasis was achieved using the Aquamantys System (Medtronic Advanced Energy,

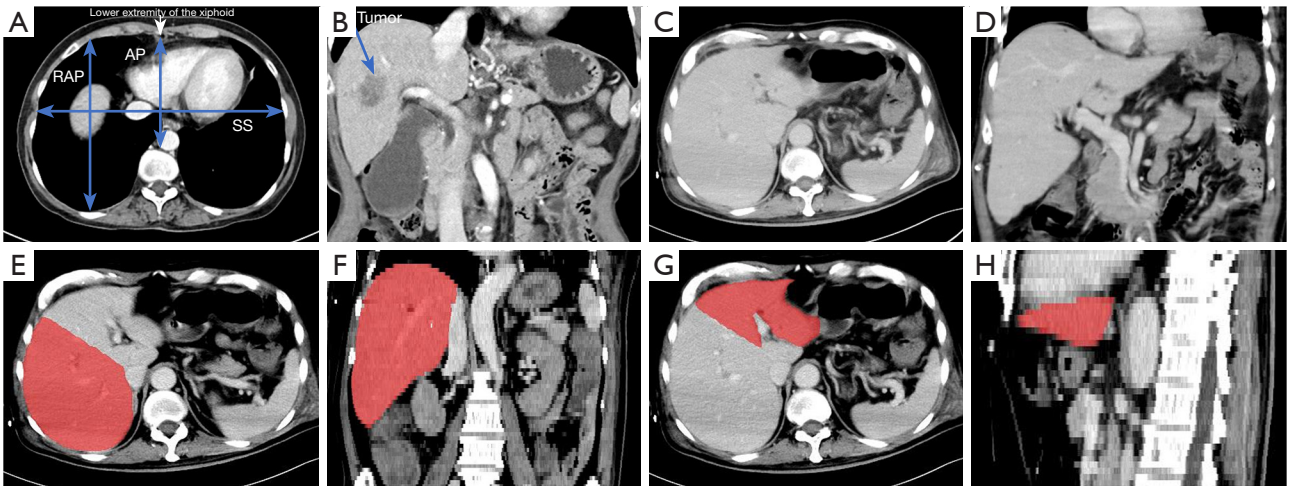


**Figure 1** Preoperative CT scan and manual CTV of the liver. (A) Morphometric measurements based on a CT scan of the recipient. RAP: the longest right anteroposterior vertical distance between the anterior and posterior parts of ribs; AP: anteroposterior distance (lower extremity of the xiphoid process to the anterior wall of vertebra); SS: side-to-side distance (the largest intraperitoneal and horizontal distance); (B) coronal abdominal CT scan of the recipient revealed a tumor located in the right anterior lobe of the liver (blue arrow); (C,D) axial and coronal abdominal CT scan of the donor; (E,F) manual CT liver volumetry of right lobe (red); (G,H) manual CT liver volumetry of left lobe (red). CT, computed tomography; CTV, computed tomography volumetry.

**Table 2** The donor-recipient matching data

| Variables | Value |
|---|---|
| Estimated GW/RAP for the whole graft (g/cm) | 120.2 |
| Estimated GW/RAP for the remnant graft (g/cm) | 70.6 |
| Actual GW/RAP after *in situ* reduction (g/cm) | 63.3 |
| Estimated GRWR for the whole graft (%) | 3.8 |
| Estimated GRWR for the remnant graft (%) | 2.2 |
| Actual GRWR after *in situ* reduction (%) | 2.0 |

GW, graft weight; RAP, right anteroposterior; GRWR, graft-recipient weight ratio.

Minneapolis, USA). The size reduction was performed by a skilled hepatobiliary surgeon and lasted 85 minutes with approximately 100 mL of blood loss. During hepatectomy, the donor was stable, and central venous pressure was maintained at 8–10 cm$H_2O$. After removal of the right posterior section (RPS), the residue graft was perfused with University of Wisconsin solution, and harvested using the routine method. Ultimately, the weight of the remaining graft was 866.8 g (GRWR: 2.0%; GW/RAP: 63.3) (*Table 2*).

The recipient underwent total hepatectomy. The reduced graft was implanted into the recipient using classical orthotopic techniques. End-to-end anastomosis of the suprahepatic and infrahepatic IVC was performed with 4-0 Prolene. A continuous 5-0 Prolene suture was used for the anastomosis of the portal vein. The arterial reconstruction was conducted using a 7-0 Prolene suture under the guidance of a microscope. End-to-end anastomosis of the bile duct was performed using 5-0 polydioxanone sutures II without a stent. After restoring liver perfusion, Doppler ultrasound showed that the blood flow velocity and resistance index of the portal vein, hepatic artery and IVC were normal. The diseased liver was incised and a grayish yellow soft mass with a 3.8-cm diameter was found in the right anterior section (RAS). Postoperative pathology revealed poorly differentiated hepatocellular carcinoma with extensive necrosis, no intravascular tumor thrombus, and no microvascular or nerve invasion.

Following LT, two doses (20 mg, days 0 and 4) of intravenous basiliximab were used to induce immunosuppression. Tacrolimus (1.5 mg, twice daily) and mycophenolate mofetil (750 mg, twice daily) were used as maintenance therapy. The PT and INR returned to normal levels on postoperative day (POD) 2 (12.6 s and 1.1, respectively), and ALT, AST, and TBil returned to near normal levels on POD 7 (49 IU/L, 56.8 IU/L, and 27.8 μmol/L, respectively; *Figure 4*). On POD 10, moderate pitting edema of both lower limbs was observed,

 

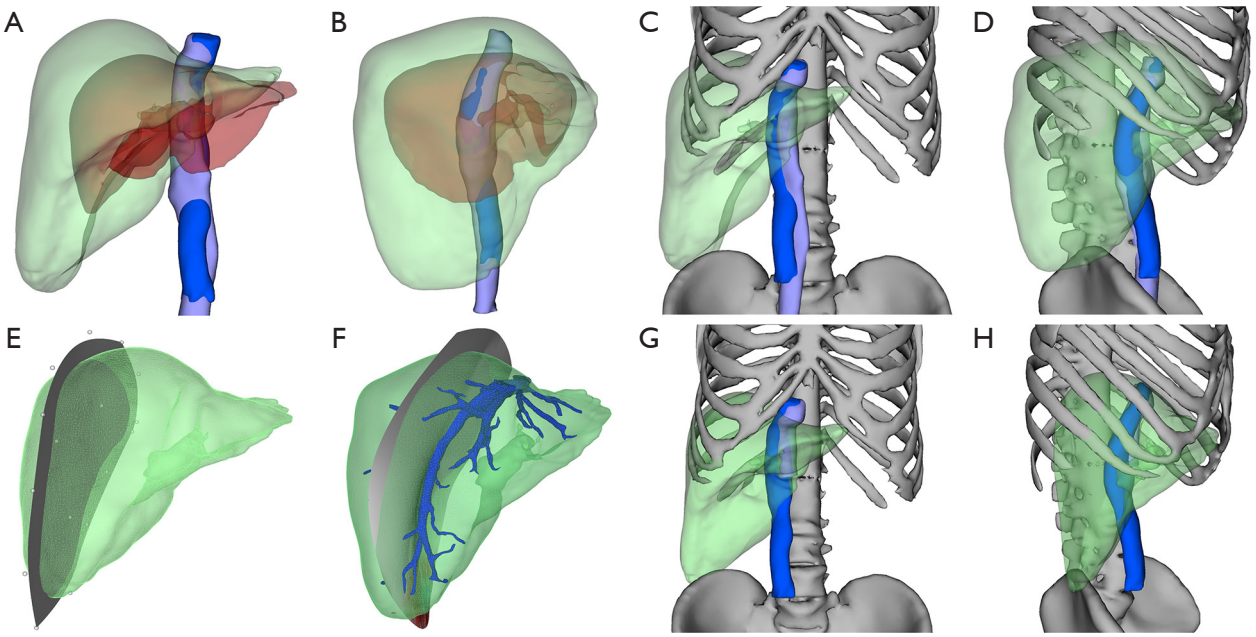


**Figure 2** Preoperative 3D reconstruction based on CT images. (A,B) 3D fusion images of the recipient liver (red) and the donor liver (green); (C,D) 3D simulation of donor liver implantation into the recipient's abdominal cavity before graft size reduction; (E,F) 3D computer-assisted design of the cutting plane of the donor liver; (G,H) 3D simulation of donor liver implantation into the recipient's abdominal cavity after graft size reduction. 3D, three-dimensional; CT, computed tomography.

accompanied by increased ascites and decreased urination. Doppler ultrasound and CT examination revealed stenosis of the retrohepatic IVC. On February 16, 2023, balloon dilatation and stent implantation of the IVC were performed (*Figure 5*). Angiography revealed rotation and distortion of the retrohepatic IVC, two stenoses in the proximal segment and thoracic 12-lumbar 1 vertebral segment, varicose vein formation in the distal IVC, and thickening of the left renal vein. A 2.5 cm × 7.5 cm bare stent was released in the thoracic 12-lumbar 1 vertebral segment, and a 3.0 cm × 7.5 cm stent was placed in the proximal segment. The stenosis of the IVC and the distal varicose vessels disappeared immediately after stent implantation. Several days later, both the lower limb edema and ascites gradually subsided. The patient recovered smoothly and was discharged on POD 30. She is currently in good condition with normal liver function, and no signs of tumor recurrence or metastasis have been observed over the 12-month follow-up period.

## Discussion

The liver is the largest solid organ in the human body, and accounts for approximately 2% of adult weight. The liver's most significant difference from other organs is that, whether it is damaged or resected, the liver weight to body weight ratio will always maintain a relatively stable level. The liver weights of individuals of different sexes and body weights differ significantly (7). Although the incidence of GRSM has been reported to be 15–25.5%, LFSS is uncommon in adult liver transplants. However, in its extreme form, LFSS can be fatal. A large graft may lead to rib compression of the liver, which can induce parenchyma necrosis or vascular obstruction, resulting in early dysfunction and even non-function (3,8). The postoperative mortality rate has been reported to be as high as 40% for large-for-size LTs, and other studies have reported decreased graft and recipient survival (2,3).

There are no official guidelines worldwide that provide a reliable estimation of the extreme LFSS risk. LFSS grafts are usually defined as a GRWR >4% in pediatric liver transplants or >2.5% in adults (9). A number of formulas have been used to predict the occurrence of LFSS, including those that use the standard liver volume, body surface area, GRWR, RAP, anteroposterior (AP) distance, and side-to-side (SS) distance (10-13). Allard *et al.* used the

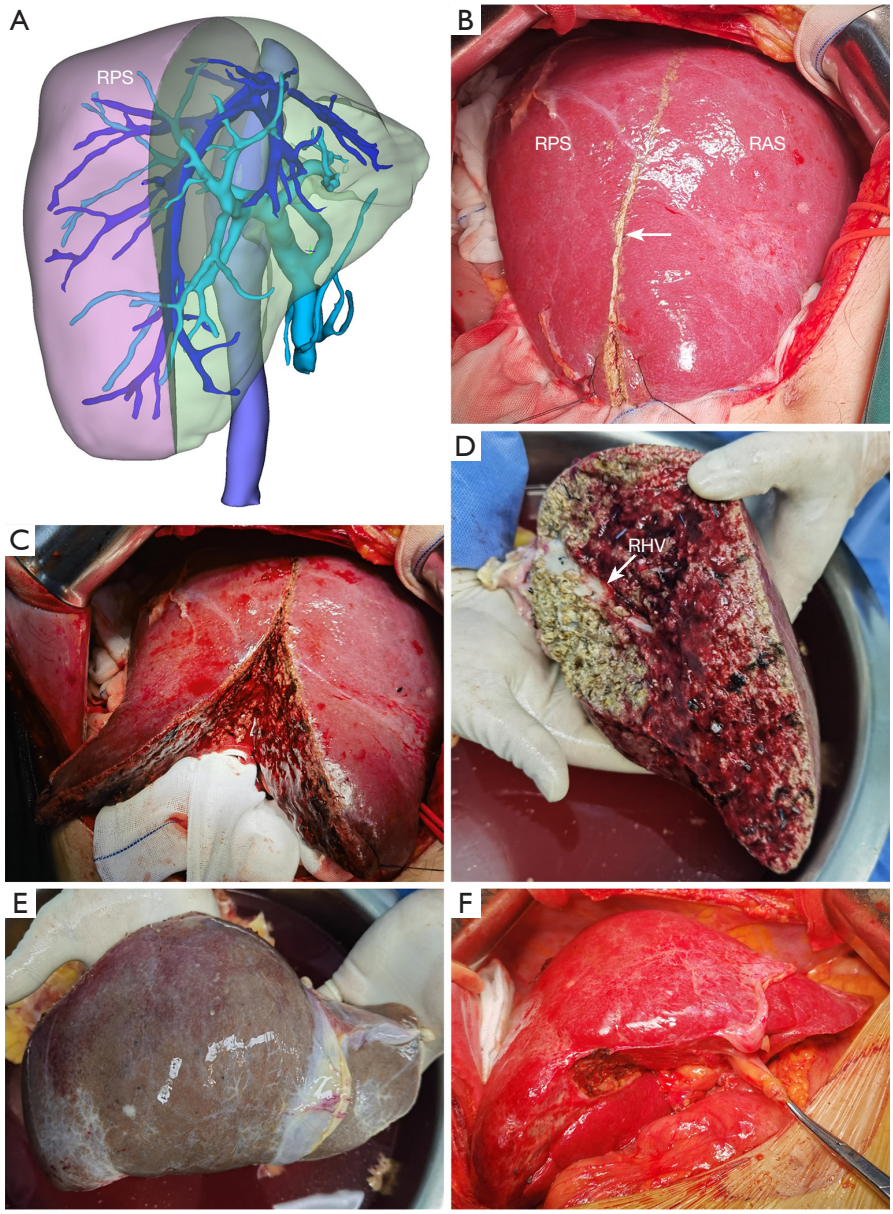


**Figure 3** Preoperative planning and surgical procedure of iRPS. (A) The RPS for resection was identified on the 3D reconstructed image; (B) the demarcation line (white arrow) between the RPS and RAS of the donor liver; (C) the *in situ* parenchymal transection of the donor liver without portal inflow occlusion; (D) RHV (white arrow) on the cutting surface of the liver graft; (E) the remaining liver graft; (F) implantation of the reduced-size liver graft into the recipient. iRPS, *in situ* right posterior segmental resection; RPS, right posterior section; 3D, three-dimensional; RAS, right anterior section; RHV, right hepatic vein.

GW/RAP to predict extreme LFSS. When the GW/RAP was 80, 100, and 120, the risk of extreme LFSS was 2.6%, 9.6%, and 29.1%, respectively. In addition, a GRWR >2.5% also significantly increases the risk of LFSS (3).

In LFSS, graft compression is usually caused by the following two factors (14): (I) the limited availability of the intra-abdominal compartment to accommodate the liver allograft; (II) the mismatch between the AP size of the allograft and the dimensions of the recipient's lower right hemithorax. The former can be treated successfully using delayed fascial closure or mesh closure (15,16), but the latter can only be treated by split liver transplantation (SLT)

 

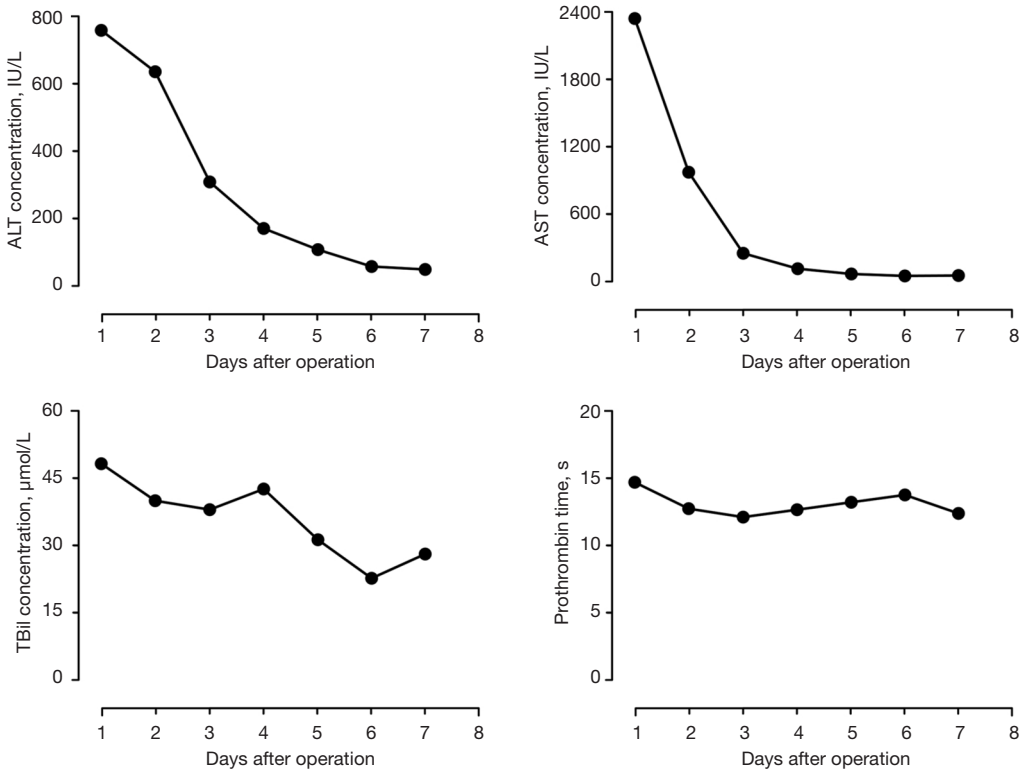


**Figure 4** Changes of the serum levels of ALT, AST, TBil, and PT during the first week following LT. ALT, alanine aminotransferase; AST, aspartate aminotransferase; TBil, total bilirubin; PT, prothrombin time; LT, liver transplantation.

or RSLT to make the graft fit the limited abdominal space of the recipient.

Delayed closure is not a good solution to liver injury caused by rib compression. Paterno *et al.* proposed a novel surgical technique named marginal costotomy to increase the space of the right abdominal cavity (17). This method significantly relieves rib compression, but it also prolongs the operation time and exacerbates surgical trauma. Given that the selection criteria for both donors and recipients in SLT are stringent and meticulously defined, RSLT may be the only solution in most cases. At present, preferential surgical approaches such as a left lobectomy or left lateral segmentectomy are often employed to address the issue of size discrepancy. However, it is very unlikely to solve the mismatch issue because rib compression mainly applies to the right liver (18). Right hemiliver resection has been suggested as a viable alternative for downsizing the graft, but there is a possibility that the residual left liver lobe could be inadequate to meet the recipient's needs and may induce SFSS (19,20). Therefore, we were of the view that right posterior sectionectomy would be the most effective and feasible way to reduce the size of the graft for this recipient.

To our knowledge, this was the first case of planned *in situ* right posterior segmental resection (iRPS). In the literature, other similar cases have used salvage operations to treat LFSS following LT (14,21). Active size reduction with meticulous surgical planning can ensure the safety of recipients with hemodynamic instability and extreme coagulation disorders. Several cases of planned *ex vivo* right posterior sectionectomy (eRPS) for graft size reduction were reported in 2022 (22). It should be noted that an eRPS results in a large transection plane that exposes the recipient to a high risk of biliary leaks and bleeding. Therefore, compared to eRPS, iRPS is a unique method with the following advantages. First, *in situ* size reduction allows the RHV to be located by intraoperative Doppler ultrasound, or the ischemic line obtained by ligating the right posterior Glissonian pedicle to be used as a surgical marker to navigate the intrahepatic transection. Second, *in situ* reduction can increase the reliability of the ligature or suture of the intrahepatic ducts, and significantly reduce

 

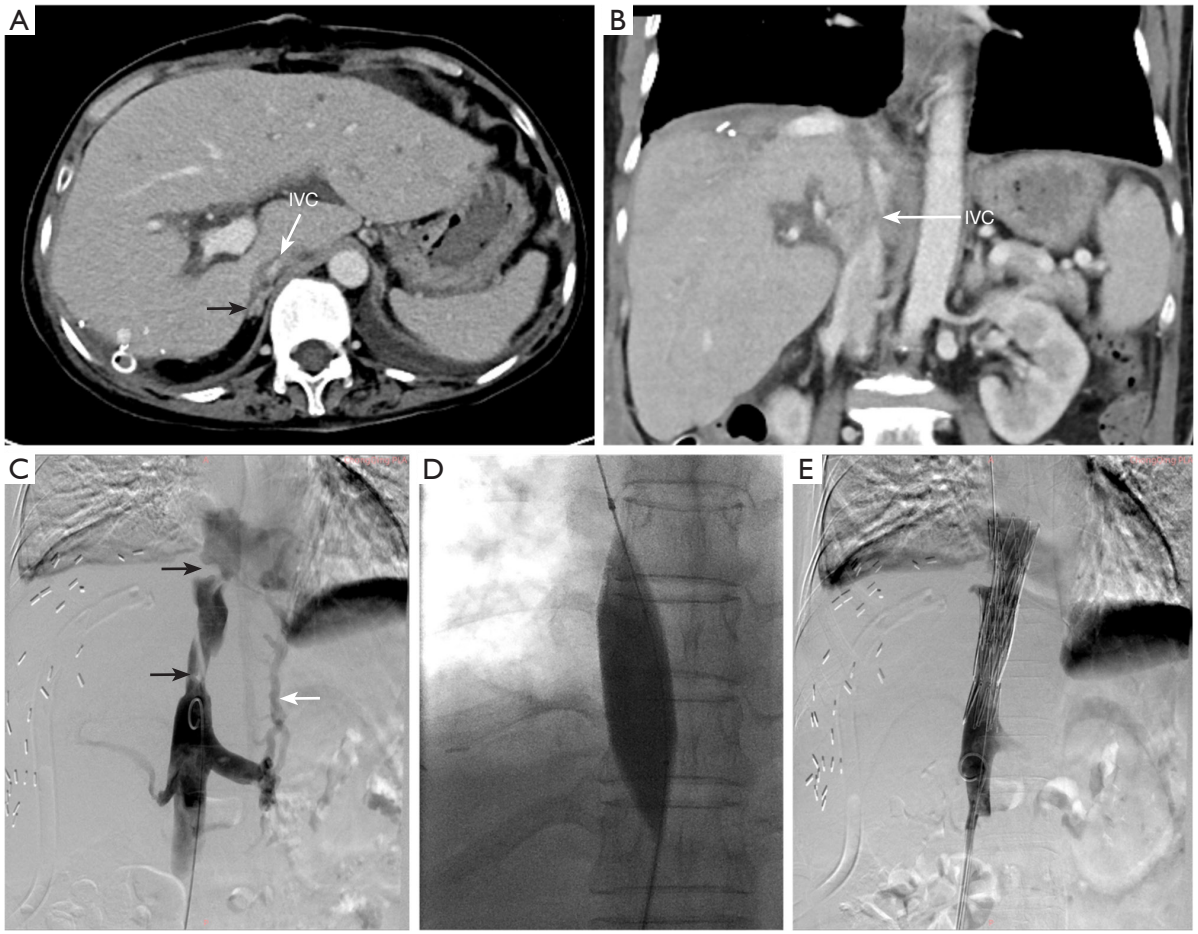


**Figure 5** IVC stenosis after liver transplantation. Postoperative abdominal CT scan: (A) stenosis of the IVC below the suprahepatic IVC anastomosis (white arrow), and engorgement of the paravertebral plexus and azygos vein (black arrows) were observed; (B) stenosis of the IVC on a coronal image (white arrow). Inferior vena cavography: (C) twisted-shape stenosis of the IVC between the supra- and infrahepatic IVC anastomosis (black arrows), and multifocal collateral flows draining into the right atrium (white arrow); (D,E) after balloon angioplasty, a 2.5 cm × 7.5 cm bare stent was released in the thoracic 12-lumbar 1 vertebral segment, and a 3.0 cm × 7.5 cm stent was placed in the proximal segment. Collateral veins disappeared. IVC, inferior vena cava; CT, computed tomography.

the incidence of bleeding or bile leakage. Finally, iRPS can significantly shorten the cold ischemia time. The disadvantages of iRPS include that the hemodynamics of the donor must remain stable during graft reduction, and intraoperative bleeding can jeopardize the procurement of other organs. Recently, Muller *et al.* performed *ex-situ* graft reduction (H67) under hypothermic oxygenated perfusion (23), and found that the technique reduces static cold storage time, which may allow for smoother reperfusion, thereby reducing graft congestion and the risk of post-implantation bleeding.

IVC stenosis is a rare but serious complication with a reported incidence of less than 1% following LT (24). It is usually observed at the surgical anastomosis site. Acute IVC stenosis results from technical factors during surgery, such as a size discrepancy between the donor and recipient IVC, or organ rotation, which leads to the kinking of the supra- or infrahepatic IVC. The piggyback technique is not recommended for recipients allocated a large-for-size liver graft, as immediate outflow obstruction has been reported in several studies as a consequence of retrohepatic IVC compression by a large graft when performing a piggyback orthotopic LT with a SS caval anastomosis (8,25). Clinical manifestations include hepatic dysfunction, ascites, pleural effusions, and swelling of the lower limbs (24).

 

In this case, the volume of the liver graft was reduced by nearly 50%. The massive size reduction of the right posterior sector led to the right rotation of the whole liver and the twisting of the IVC. Therefore, to prevent the kinking of the IVC, end-to-end anastomosis of the supra- or infrahepatic IVC should be performed when the residual liver graft has been placed in a natural and stable position in the recipient's abdominal cavity. Rotating the graft and alleviating IVC compression through mechanical interventions (e.g., prosthesis, pads, and filled gloves) has also been reported (8). Another technical option is to fashion two caval anastomoses, one above and one below the large graft (using the "passing loop" technique) (25). Endovascular interventions are usually used to manage IVC stenosis following LT. Stent placement is effective and has long-term patency for treating IVC stenosis (26).

The major limitation of this study is that we only provided descriptive data for this patient. Due to the small sample size of this study, we could not compare the effect of using 3D computer-assisted planning between an experimental group and a control group, which impedes our capacity to reach a firm consensus as to the benefits of this technology compared to those of existing standards of care. Our 3D model simulates the patient's abdominal cavity; however, it does not reflect the actual elasticity of the ribs, abdominal wall, the diaphragm, and other adjacent organs. This raises a practical question as to whether real allografts will fit into recipients, and surgeons must take into account the elasticity of the adjacent organs and muscular structures of the liver fossa, as well as the biomechanical effects they impose on the liver graft, when making decisions based on our 3D model. Currently, we are developing new 3D reconstruction software offering biomechanical analysis, which will enable surgeons to more accurately assess the compatibility of the donor liver with the recipient's abdominal cavity, allowing for the further optimization of preoperative surgical plans.

## Conclusions

In conclusion, iRPS is a simple and effective method to prevent LFSS after adult LT, especially if there is a size discrepancy between the donor liver AP dimensions and the recipient's lower right hemithorax. The 3D simulation implanting model is very useful for accurately assessing the compatibility of the donor liver with the recipient's abdominal cavity prior to LT.

## Acknowledgments

*Funding:* This work was funded by a key joint project of Chongqing Health Commission and Science and Technology Bureau (No. 2024ZDXM007 to G.C.), a grant from the National Natural Science Foundation of China (No. 81570594 to G.C.), and a key medical research project of "Artificial Intelligence Plus" (No. ZXAIZD003 to G.C.).

## Footnote

*Reporting Checklist:* The authors have completed the CARE reporting checklist. Available at https://qims.amegroups.com/article/view/10.21037/qims-24-507/rc

*Conflicts of Interest:* All authors have completed the ICMJE uniform disclosure form (available at https://qims.amegroups.com/article/view/10.21037/qims-24-507/coif). The authors have no conflicts of interest to declare.

*Ethical Statement:* The authors are accountable for all aspects of the work in ensuring that questions related to the accuracy or integrity of any part of the work are appropriately investigated and resolved. This study was a retrospective investigation. All procedures performed in this study were in accordance with the ethical standards of the institutional and/or national research committee(s) and with the Helsinki Declaration (as revised in 2013). Written informed consent was obtained from the patient for the publication of this case report and any accompanying images. A copy of the written consent is available for review by the editorial office of this journal.



## References

1. Ersoy Z, Kaplan S, Ozdemirkan A, Torgay A, Arslan G, Pirat A, Haberal M. Effect of Graft Weight to Recipient Body Weight Ratio on Hemodynamic and Metabolic

Parameters in Pediatric Liver Transplant: A Retrospective Analysis. Exp Clin Transplant 2017;15:53-6.
2. Addeo P, Noblet V, Naegel B, Bachellier P. Large-for-Size Orthotopic Liver Transplantation: a Systematic Review of Definitions, Outcomes, and Solutions. J Gastrointest Surg 2020;24:1192-200.
3. Allard MA, Lopes F, Frosio F, Golse N, Sa Cunha A, Cherqui D, Castaing D, Adam R, Vibert E. Extreme large-for-size syndrome after adult liver transplantation: A model for predicting a potentially lethal complication. Liver Transpl 2017;23:1294-304.
4. Menon KV, Hakeem AR, Heaton ND. Review article: liver transplantation for hepatocellular carcinoma - a critical appraisal of the current worldwide listing criteria. Aliment Pharmacol Ther 2014;40:893-902.
5. Lemke AJ, Brinkmann MJ, Schott T, Niehues SM, Settmacher U, Neuhaus P, Felix R. Living donor right liver lobes: preoperative CT volumetric measurement for calculation of intraoperative weight and volume. Radiology 2006;240:736-42.
6. Tamulevicius M, Oezcelik A, Koitka S, Theysohn JM, Hoyer DP, Farzaliyev F, Haubold J, Nensa F, Treckmann J, Malamutmann E. Preoperative Computed Tomography Volumetry and Graft Weight Estimation of Left Lateral Segment in Pediatric Living Donor Liver Transplant. Exp Clin Transplant 2023;21:831-6.
7. Michalopoulos GK. Hepatostat: Liver regeneration and normal liver tissue maintenance. Hepatology 2017;65:1384-92.
8. Lim C, Osseis M, Tudisco A, Lahat E, Sotirov D, Salloum C, Azoulay D. Hepatic venous outflow obstruction after whole liver transplantation of large-for-size graft: versatile intra-operative management. Ann Hepatobiliary Pancreat Surg 2018;22:321-5.
9. Levesque E, Duclos J, Ciacio O, Adam R, Castaing D, Vibert E. Influence of larger graft weight to recipient weight on the post-liver transplantation course. Clin Transplant 2013;27:239-47.
10. Kasahara M, Sakamoto S, Umeshita K, Uemoto S. Effect of graft size matching on pediatric living-donor liver transplantation in Japan. Exp Clin Transplant 2014;12 Suppl 1:1-4.
11. Croome KP, Lee DD, Saucedo-Crespo H, Burns JM, Nguyen JH, Perry DK, Taner CB. A novel objective method for deceased donor and recipient size matching in liver transplantation. Liver Transpl 2015;21:1471-7.
12. Fukazawa K, Nishida S, Volsky A, Tzakis AG, Pretto EA Jr. Body surface area index predicts outcome in orthotopic liver transplantation. J Hepatobiliary Pancreat Sci 2011;18:216-25.
13. Jacob M, Saif R, Reddy J, Medappil N, Asthana S, Lochan R. Extreme large-for-size syndrome after adult liver transplantation: A model for predicting a potentially lethal complication. Liver Transpl 2018;24:442-3.
14. Nagatsu A, Yoshizumi T, Ikegami T, Harimoto N, Harada N, Soejima Y, Taketomi A, Maehara Y. In Situ Posterior Graft Segmentectomy for Large-for-Size Syndrome in Deceased Donor Liver Transplantation in Adults: A Case Report. Transplant Proc 2017;49:1199-201.
15. Brustia R, Perdigao F, Sepulveda A, Schielke A, Conti F, Scatton O. Negative wound therapy to manage large-for-size liver graft mismatch. Clin Res Hepatol Gastroenterol 2015;39:552-4.
16. Sakamoto S, Uchida H, Fukuda A, Kasahara M. Armamentarium to overcome "large-for-size" scenarios in pediatric liver transplantation: Graft reduction or delayed abdominal wall closure? Pediatr Transplant 2022;26:e14177.
17. Paterno F, Amin A, Lunsford KE, Brown LG, Pyrsopoulos N, Lee ES, Guarrera JV. Marginal Costotomy: A Novel Surgical Technique to Rescue from "Large-for-Size Syndrome" in Liver Transplantation. Liver Transpl 2022;28:317-20.
18. Kim YM, Kwak BJ, Shim DJ, Kwon YK, Yoon YC. In Situ Left Lateral Sectionectomy in Deceased Donor Liver Transplantation: Could This Be Another Solution for a Large-for-Size Graft? A Case Report. Transplant Proc 2019;51:3116-9.
19. He D, Pu X, Jiang L. How to Choose the Optimal Surgical Strategy to Predict and Prevent LFSS Following Liver Transplantation? Transpl Int 2022;35:10805.
20. Minami T, Ebata T, Yokoyama Y, Igami T, Mizuno T, Yamaguchi J, Onoe S, Watanabe N, Nagino M. Study on the Segmentation of the Right Posterior Sector of the Liver. World J Surg 2020;44:896-901.
21. Kim EY, Yoon YC. Performing a Right Hemihepatectomy Sequentially After Deceased Donor Liver Transplantation--The Solution for a Large-for-size Graft: A Case Report. Transplant Proc 2015;47:3023-6.
22. Pu X, He D, Liao A, Yang J, Lv T, Yan L, Yang J, Wu H, Jiang L. A Novel Strategy for Preventing Posttransplant Large-For-Size Syndrome in Adult Liver Transplant Recipients: A Pilot Study. Transpl Int 2021;35:10177.
23. Muller X, Rossignol G, Mohkam K, Mabrut JY. Ex-situ graft reduction (H67) during hypothermic oxygenated perfusion to prevent large-for-size syndrome in liver

 

transplantation-A technical report. Clin Transplant 2023;37:e14995.
24. Choi Y, Kim JH, Jeon UB, Jang JY, Kim TU, Ryu H. Inferior Vena Cava Stenosis Following Orthotopic Liver Transplantation: Differentiating Points from False Positives. J Korean Soc Radiol 2023;84:713-8.
25. Eldeen FZ, Lee CF, Lee CS, Chan KM, Lee WC. "Passing loop" technique: a new modification of the piggyback technique tailored to voluminous liver grafts--case report. Transplant Proc 2013;45:831-2.
26. Lee JM, Ko GY, Sung KB, Gwon DI, Yoon HK, Lee SG. Long-term efficacy of stent placement for treating inferior vena cava stenosis following liver transplantation. Liver Transpl 2010;16:513-9.

**Cite this article as:** Zhang S, Zhou B, Chen P, Chen G. *In situ* right posterior sectionectomy during liver procurement based on preoperative 3D planning to prevent extreme large-for-size syndrome in adult-to-adult liver transplantation: a case report. Quant Imaging Med Surg 2024;14(12):9552-9562. doi: 10.21037/qims-24-507